Uranyl-Tc(VII)/Tc(V) hybrid clusters

Journal:	*ChemComm*
Manuscript ID	CC-COM-04-2024-001726.R1
Article Type:	Communication

COMMUNICATION

Uranyl-Tc(VII)/Tc(V) hybrid clusters

Mohammad Shohel[a] and May Nyman* [a]

Received 00th January 20xx,
Accepted 00th January 20xx

DOI: 10.1039/x0xx00000x

Pertechnetate ($^{99}Tc^{VII}O_4^-$), reduced Tc, and actinides co-exist in spent nuclear fuel and legacy wastes. They co-transport in fuel reprocessing and waste disposal scenarios, necessitating an understanding of co-speciation. Here we report five new molecular cluster/framework structures with pentameric and tetrameric uranyl building units decorated by TcO_4^-/ReO_4^- oxoanions, or fused with the reduced technetyl cation Tc(V)O. The latter, obtained by Tc auto-reduction (without intentional introduction of a reducing environment), broadens the basis for Tc-reduction and the burgeoning polyoxometalate-like behavior of technetium.

Technetium-99 is a high-yield and long-lived decay product of U-235 fission, which is utilized in nuclear energy and nuclear weapons. Technetium poses a challenge during solvent-extraction reprocessing of spent nuclear fuel, specifically by co-mobilizing with actinides and other elements, hampering efficient separation.[1] One possible mechanism of this co-extraction is coordination of pertechnetate (TcO_4^-) with actinides and other metal ions present in the spent nuclear fuel.[2] A growing number of crystal structures evidence direct coordination of pertechnetate/perrhenate (ReO_4^-, a TcO_4^- surrogate) with actinides and other metals present in spent nuclear fuel as process chemicals or fission products (i.e. Zr).[3] We are interested in expanding the library of metal-TcO_4^-/ReO_4^- coordination compounds (along with related solution characterization) to deepen fundamental knowledge of Tc behaviour in the range of relevant complex matrices.

Legacy nuclear wastes stored in Hanford WA and the Savannah River Site is one such complex matrix. Due to Tc's persistence ($T_{1/2}$ = 2.11x10^5 y), radioactivity (β = 292 keV), variable redox states, and high mobility in the environment via solubility or volatilization (i.e. as Tc_2O_7), Tc-99 is one of the greatest challenges in nuclear waste management and disposal.[4] In the highly alkaline tank waste environments, Tc is expected to exist as the fully oxidized TcO_4^- (pertechnetate) species[5]. Yet, owed to presence of organics coupled with radiolysis and catalytic activity, low valence/reduced Tc species have been readily identified in the Hanford Tank wastes.[6] However, the speciation of low valence Tc and how it affects mobility is still not well-understood.

Uranyl hybrid materials composed of UO_2^{2+} plus organic or inorganic ligands or linkers have gained attention in the last two decades. Interest in hybrid uranyl materials ranges from designing uranyl metal organic frameworks (MOFs), understanding crystal growth of U(VI) species from solution,[7] and studying secondary building units (SBU) of UO_2^{2+} that are analogous to structural motifs observed in uranyl minerals.[8] Nuclearity and topology of uranyl SBUs in hybrid materials/minerals varies from finite nodes (monomer, dimer, trimer, tetramer, etc.) to infinite chains and sheets, where the multiply-bound oxos of the linear uranyl unit have strong structure-directing effects, favoring low-dimensional assemblies. Isolating SBUs as soluble molecular clusters (instead of insoluble lattices) is challenging, surmised from the paucity of published structures and solution phase studies.[3a, 9] Prior-reported uranyl-hybrid materials exploit carboxylates, carboxyphosphonates, and halides as ligands; partly motivated by their prevalence in environmental, reprocessing, or waste storage environments.[8b, 10] Uranyls linked by inorganic ligands (carbonate,[11] phosphate,[12] sulfate,[13] selenate,[13a] vanadate,[9b] molybdate,[14] silicate[15]) expands uranyl solid-state chemistry and understanding of complex mineral topologies. Perrhenate, isostructural with the above-mentioned tetrahedral oxoanions, also has demonstrated uranyl-ligation in molecular forms with phosphonate heteroligands,[16] in layered materials, and ReO_4^--capped flat dimers and trimers[3a]. Despite its relevancy in spent nuclear fuel reprocessing and tank waste solutions, there are fewer reported structures featuring uranyl-pertechnetate coordination.[2a] Moreover, amongst the growing collection of Tc-heterometal structures with metals from across the periodic table,[17] none feature reduced Tc species.

Here we present five pentameric/tetrameric uranyl cluster compounds featuring direct coordination between uranyl and TcO_4^-/ReO_4^-, and the reduced technetium oxocation $Tc(V)O^{3+}$. Isolation of Tc^V-complexes is still relatively rare, and usually obtained in a multiplex of conditions conducive to reduction including air-free, highly acidic, and/or radiation environments

---

[a] *Department of Chemistry, Oregon State University, Corvallis, OR-97331, USA.*

† Footnotes relating to the title and/or authors should appear here.

Electronic Supplementary Information (ESI) available: [CCDC 2332264-2332268] contains CIF files of structures. Additional figures and details of chemical characterization are available in SI]. See DOI: 10.1039/x0xx00000x (i.e. applied photolysis or external radioactivity).[18] On the other hand, our syntheses were performed without the exclusion of oxygen, intentional photoreduction, nor addition of acid, beyond that of the pertechnic acid, implying the community needs to carefully consider Tc reduction mechanisms.

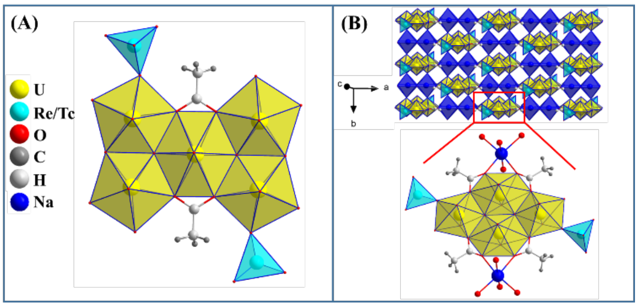

Figure 1. Polyhedral representation of **A) U_5Re_2/U_5Tc_2** molecular cluster and (**B**) **U_4Re_2/U_4Tc_2** 2D framework and the tetrameric unit (inset).

To synthesize the reported compounds, we dissolved uranyl acetate in perrhenic/pertechnic acid solutions, followed by crystallization via evaporation (details in SI). All described molecules contain the linear axial uranyl cation (UO_2^{2+}), exhibiting hexagonal or pentagonal bipyramidal geometry. The $U{\equiv}O_{yl}$ bond distances are 1.756(8)-1.792(5) Å and equatorial U-O bonds are 2.217(2)- 2.592(4) Å, with axial oxygen-ligands from perrhenate, pertechnetate, acetate, water, Tc(V)O_5, or adjoining UO_2^{2+}. The Re-O bond lengths of the ReO_4^-/TcO_4^- tetrahedral oxoanions range between 1.709(5)-1.739(5) Å, and the Tc-O bond lengths are slightly shorter, 1.689(8)-1.732(7) Å. Details of SCXRD analysis and selected crystallographic information is summarized in **Table S1**. **Table S2** compiles relevant bond valence sum (BVS) calculations. The calculated average BVS values for fully occupied U(VI), Re(VII) and Tc(VII) sites are 6.06, 6.86 and 6.65, respectively. Bond distances and BVS for Tc(V) is discussed later.

U_5Re_2 and **U_5Tc_2** (moiety formulae $[(UO_2)_5(O)_2(OH)_2(H_2O)_6(MO_4)_2(CH_3COO)_2]$ M=Re, Tc) are isostructural flat pentameric clusters composed of four mutually edge-sharing uranyl pentagonal bipyramids surrounding a uranyl hexagonal bipyramid (**figure 1A**). The pentamer is additionally decorated by acetate and TcO_4^-/ReO_4^- ions. The central hexagonal bipyramid, coordinated by two μ_3-oxo and four oxygens from two bidentate acetates is equatorially distorted. The acetate edge (measured by the oxygen-to-oxygen distance) is 2.1675(6) Å, while the other edges shared with uranyl pentagonal bipyramids are considerably longer, ~2.61-2.62 Å. The two μ_3-oxos connect to two uranyl pentagonal bipyramid dimers on each side, which flank the central hexagonal bipyramid. The uranyl pentagonal bipyramids are also coordinated to oxygen atoms from μ_2-oxo, H_2O and acetate in their equatorial plane. Two of the four uranyl pentagonal bipyramids are also coordinated to oxygen from decorating perrhenate/pertechnetate. **Figure S1** shows the packing of the neutral clusters in the crystalline lattice. This $(UO_2)_5$ pentamer topology was observed prior, linked by sulfobenzoate[19], phosphate[10a] and phosphonoacetate.[20] Notably, all of these prior-reported pentamers also exhibit distortion of the central hexagonal bipyramid, invoked by coordination of a bridging oxoanion that define the short edges. However, **U_5Re_2** and **U_5Tc_2** are the first example of the $(UO_2)_5$ unit as a molecular cluster instead of within a framework, allowing solution phase studies.

U_4Re_2 and **U_4Tc_2** are nearly isostructural 2D frameworks built of the tetrameric uranyl SBU and a moiety formula of $[(UO_2)_4(O)_2(H_2O)_2(MO_4)_2(CH_3COO)_4Na_2(H_2O)_2]$ (M=Re/Tc). These crystals are obtained as a minor product alongside **U_5Re_2/U_5Tc_2**, since the Na is incorporated into the reaction solution presumably via leaching of the glass vials. Intentional introduction of Na-salt increases the yield of this phase, but there is always a mixture of the pentamer and tetramer phases. The tetramer is composed of two mutually edge-sharing uranyl hexagonal bipyramids and two uranyl pentagonal bipyramids (**figure 1B**). The two hexagonal bipyramids link via two μ_3-oxos, each of which connect to the uranyl pentagonal bipyramids that flank the hexagons. The uranyl pentagonal bipyramids are also coordinated to oxygens from acetate, H_2O and TcO_4^-/ReO_4^-. The ReO_4^- are disordered in the structure; each rhenium site is located over three different positions with 0.50, 0.25 and 0.25 occupancy. However, the Tc site in **U_5Tc_2** exhibited no disorder. The uranyl tetramer clusters are linked along the *a*-axis via $Na_2(H_2O)_2$-dimers, and along the b-direction via U-O_{yl}-Na-O_{yl}-Na infinite chains (Na-OH_2 and Na-O_{yl} ~2.4 Å). Acetates that coordinate the hexagonal uranyl bipyramids also bridge to Na with Na-$O_{acetate}$ ~2.3 Å. Another view of the 2d-framework is shown in **figure S2**. Hybrid framework materials featuring the uranyl tetramer $(UO_2)_4$ were described prior, capped with sulfonate, carboxylate and cucurbit ligands.[21] In addition, Felton *et al.* recently reported the isolated tetramer capped with a sulfonate ligand.[9b]

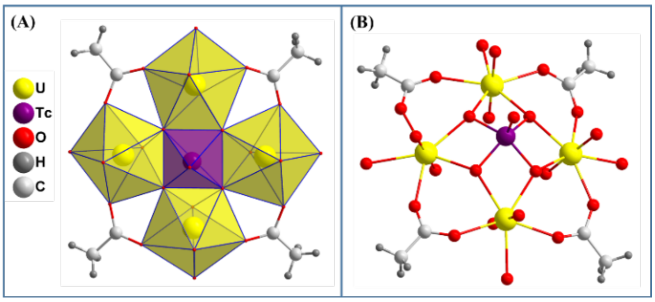

Figure 2. (**A**) Polyhedral representation of **U_4Tc** molecular cluster and (**B**) Ball-stick representation of **U_4Tc** molecular cluster.

U_4Tc is a unique pentameric molecular cluster composed of four uranyl pentagonal bipyramids that share edges with a square-pyramidal $Tc^V{=}O$ via μ_3-oxos (**figure 2**, Tc-O bond distances 1.877(8) – 1.905(7) Å). These same μ_3-oxos bond to U^{VI} with a bond distance of ~2.334(8) - 2.357(8) Å, and the uranyl pentagonal bipyramids are further coordinated by a terminal H_2O (U-O_{water} ~ 2.5 Å), and two bridging acetates (U-$O_{acetate}$ ~ 2.3-2.4 Å). The out-of-plane coordination of $Tc^V{=}O$ gives rise to an umbrella-shape, in contrast to the flat clusters described in this paper. In the extended lattice, the **U_4Tc** clusters are arranged approximately parallel in the *ac* plane, with alternating orientation of Tc=O bond (**figure S3**). Isolated H_3O^+/H_2O molecules sit between the clusters and associate via H-bonding with UO_2^{2+} and H_2O coordinated to them, with O---O distances of 2.667(2) to 2.960(3). The moiety formula for **U_4Tc** is $[(UO_2)_4(TcO)(O)_4(CH_3COO)_4\ (H_2O)_4{\cdot}H_3O,H_2O]$, and based on bond valence sum calculations (BVS, **Table S2**), the H_3O^+ is necessary for charge-balance. This is a reasonable presumption because 1) there is precedence for charge-balancing H_3O^+ with Tc-clusters,[18b] 2) $HTcO_4$ co-crystallizes with **U_4Tc**, an indication of the high acid-content of the reaction solution.

The Tc^V=O square-pyramidal unit was reported recently, but with chelating organic ligands (i.e. catecholate).[22] Francesconi prior demonstrated chemical or photoreduction of TcO_4^- to Tc^V=O, followed by incorporation into tungstate polyoxometalates, enabled by the structural similarity of the Tc^V=O and W^{VI}=O units.[18a, 23] However, both tungstyl and technetyl are in distorted octahedral coordination within the POMs, instead of square planar coordination observed here. The reduction of Tc^{VII} to Tc^V was not premeditated, but auto-reduction of pertechnetate is not unprecedented, even without the presence of organics such as the acetate in this reported synthesis. The Tc=O and average Tc-$O_{equatorial}$ bond lengths in this study are 1.656 Å and 1.896 Å, respectively, consistent with the previously reported $Tc(V)O_5$ with organic ligation (**Table S3**).[22] Likewise, the BVS value for Tc(V) is consistent with the 5+ oxidation state (5.35, **Table S2**). Additional evidence for pentavalent Tc is the different color of these crystals. Clusters containing uranyl and TcO_4^- are generally orange or yellow, while **U_4Tc** is dark yellow with contribution form the red-brown color of Tc^V=O.

We used SAXS to investigate the stability/lability and crystallization pathways of the various reported clusters in water, with the caveat of their co-crystallization, and therefore presence of mixed species. Nonetheless, they are similar sizes and shapes in the crystallized form, and should exhibit similar assembly pathways. Analysis on both the mother liquor and crystals redissolved in water showed relatively weak scattering and sizes consistent with monomers instead of intact clusters, likely due to the acidity of these solutions (**figure S4**). For comparison, we have simulated the scattering of ReO_4^- and a Re_2O_7 dimer, and the scattering observed in these aqueous solutions suggests comparably-sized species. In addition to water, the mixed crystalline materials were moderately soluble in acetonitrile, enabling additional solution characterization. SAXS of the crystals dissolved in acetonitrile (**figure 3**) also indicate the presence of species smaller than a pentamer or tetramer, based on comparison of the simulated scattering to the experimental scattering. To further investigate the species dissolved in acetonitrile, we simulated scattering from hypothetical fragments of **U_5Re_2/U_5Tc_2**. The experimental scattering matches quite well to the simulated scattering of a uranyl dimer coordinated with a single TcO_4^-/ReO_4^- (**Figure 3**, inset). This suggests that 1) larger molecular cluster present in solid state dissociate to smaller fragments in acetonitrile, or 2) only smaller fragments are soluble in acetonitrile. In addition, the mixed $U_5Tc_2/U_4Tc_2/U_4Tc$ evidences aggregation or polymerization, based on the upswing of intensity of this SAXS curve at q<0.03 $Å^{-1}$.

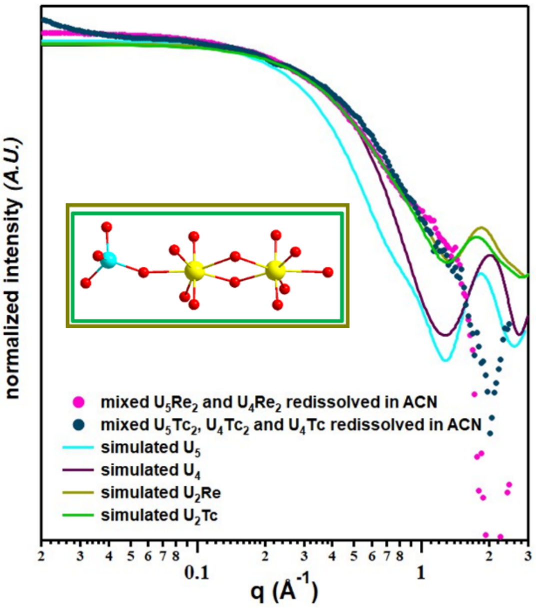

Figure 3. SAXS of co-crystallized mixtures, dissolved in acetonitrile. Inset shows a simulated uranyl dimer coordinated with a single ReO_4/TcO_4, corresponding with simulated SAXS curves. This unit is a fragment of **U_5Re_2/U_5Tc_2**, and shows the best match to the experimental scattering.

We performed additional chemical characterization on bulk crystalline materials using FTIR, Raman spectroscopy, PXRD and SEM-EDS. For the Tc-99-containing materials, the characterization was limited to Raman spectroscopy and SEM-EDS, due to regulatory limitations. All these characterizations are representative of mixed crystalline materials, and are summarized in the SI.

This work contributes towards understanding coordination between oxoanionic/reduced Tc-99 and UO_2^{2+} species, which co-exist in spent nuclear fuel/legacy waste. The SAXS (especially of the reaction solutions) indicates the clusters do not necessarily assemble in aqueous solution prior to crystallization, nor can they redissolve intact in aqueous solution. Rather, we expect they crystallize in the solid phase in a manner more similar to that described as 'classical nucleation';[24] i.e. monomer-by-monomer growth. This has been suggested prior for other clusters that crystallize from acidic media, such as the Cr-Al polycations, where assembly at air-water interfaces enables crystallization.[25] Nonetheless, **U_4Tc** is the first-reported heterometallic oxocluster featuring connectivity between actinyl and Tc^V=O, building on the foundation laid by Francesconi who established $(Tc,Re)^V$=O substituted POMs.[18a, 23] The Tc^V=O unit was obtained via auto-reduction of $Tc^{VII}O_4^-$, a phenomenon that could be further exploited to develop the emergent oxocluster chemistry of technetium, established by German et al.[18b] Finally, the curvature observed in the **U_4Tc** unit (directed by square-pyramidal Tc^V=O) suggests it can be joined into larger cages via ditopic ligands, fusion of the umbrella-shaped units, or linkage through additional metals. This is the focus of future studies, in addition to obtaining **U_4Tc** in purer forms to allow more complete solution characterization and manipulation.

Conflicts of interest

There are no conflicts to declare.

Notes and references

This study was supported by the DOE, NNSA under Award DE-NA0003763. Tc-99 was supplied by the U.S. DOE Isotope Program, managed by the Office of Isotope R&D and Production. *Caution!!* Radioactive materials were used: ^{99}Tc (β-emitter) and ^{238}U (α-emitter). Experiments were conducted by trained personnel in a licensed research facility with special precautions taken towards the handling, monitoring, and disposal of radioactive materials.

1. K. George, A. J. Masters, F. R. Livens, M. J. Sarsfield, R. J. Taylor and C. A. Sharrad, *Hydrometallurgy*, 2022, **211**, 105892.
2. a) M. J. Sarsfield, A. D. Sutton, I. May, G. H. John, C. Sharrad and M. Helliwell, *Chem Commun*, 2004; b) A. D. Sutton, I. May, C. A. Sharrad, M. J. Sarsfield and M. Helliwell, *Dalton Transactions*, 2006, 5734-5742.
3. a) O. V. Karimova and P. C. Burns, *Inorganic Chemistry*, 2007, **46**, 10108-10113; b) A. M. Fedosseev, N. A. Budantseva, M. S. Grigoriev, K. E. Guerman and J.-C. Krupa, *Radiochim Acta*, 2003, **91**, 147-152; c) M. Shohel, J. Bustos, G. D. Stroscio, A. Sarkar and M. Nyman, *Inorg Chem*, 2023, **62**, 10450-10460; d) M. Shohel, J. Bustos, A. Roseborough and M. Nyman, *Chem Eur J*, 2024, **30**, e202303218; e) M. Shohel, A. K. Sockwell, A. E. Hixon and M. Nyman, *InorgChem*, 2024, **63**, 2044-2052; f) E. Strub, D. Grödler, D. Zaratti, C. Yong, L. Dünnebier, S. Bazhenova, M. Roca Jungfer, M. Breugst and M. Zegke, *Chem Eur J*, 2024, **30**, e202400131.
4. T. Levitskaia, S. Bryan, S. Chatterjee, J. Crum, R. Peterson, B. Riley, J. Serne and J. H. Westsik, Jr., WM2016: 42 Annual Waste Management Symposium, United States, 2016.
5. G. K. Schweitzer and L. L. Pesterfield*, The aqueous chemistry of the elements*, OUP USA, 2010.
6. a) S. Chatterjee, V. E. Holfeltz, G. B. Hall, I. E. Johnson, E. D. Walter, S. Lee, B. Reinhart, W. W. Lukens, N. P. Machara and T. G. Levitskaia, *Anal Chem*, 2020, **92**, 13961-13970; b) R. J. Serne, B. M. Rapko and I. L. Pegg, *Technetium Inventory, Distribution, and Speciation in Hanford Tanks*, United States, 2014.
7. a) P. Li, N. A. Vermeulen, C. D. Malliakas, D. A. Gómez-Gualdrón, A. J. Howarth, B. L. Mehdi, A. Dohnalkova, N. D. Browning, M. O'Keeffe and O. K. Farha, *Science*, 2017, **356**, 624-627; bS. L. Hanna and O. K. Farha, *Chem Sci*, 2023, **14**, 4219-4229.
8. a) P. C. Burns, *The Canad Mineral*, 2005, **43**, 1839-1894; b) M. B. Andrews and C. L. Cahill, *Chem Rev*, 2013, **113**, 1121-1136.
9. a) T. A. Kohlgruber, G. A. Senchyk, V. G. Rodriguez, S. A. Mackley, F. Dal Bo, S. M. Aksenov, J. E. S. Szymanowski, G. E. Sigmon, A. G. Oliver and P. C. Burns, *Inorg Chem*, 2021, **60**, 3355-3364; b) D. E. Felton, T. A. Kohlgruber, Z. D. Tucker, E. M. Gulotty, B. L. Ashfeld and P. C. Burns, *Cryst Growth Des*, 2023, **11**, 8311–8318.
10. a) N. P. Deifel, K. T. Holman and C. L. Cahill, *Chem Comm*, 2008, 6037-6038; b) T. Loiseau, I. Mihalcea, N. Henry and C. Volkringer, *Coord Chem Rev*, 2014, **266-267**, 69-109; c) N. P. Deifel and C. L. Cahill, *Comptes Rendus Chimie*, 2010, **13**, 747-754.
11. V. V. Gurzhiy, S. A. Kalashnikova, I. V. Kuporev and J. Plášil, *Crystals*, 2021, **11**, 704.
12. a) E. M. Wylie, C. M. Dawes and P. C. Burns, *J Sol State Chem*, 2012, **196**, 482-488; b) E. M. Villa, C. J. Marr, L. J. Jouffret, E. V. Alekseev, W. Depmeier and T. E. Albrecht-Schmitt, *Inorg Chem*, 2012, **51**, 6548-6558; c) V. Kocevski, C. A. Juillerat, E. E. Moore, H.-C. zur Loye and T. M. Besmann, *Cryst Growth Des*, 2019, **19**, 966-975.
13. a) J. Ling, G. E. Sigmon, M. Ward, N. Roback and P. Carman Burns, *Zeitschrift für Kristallographie – Crystalline Materials*, 2010, **225**, 230-239; b) T. Z. Forbes, V. Goss, M. Jain and P. C. Burns, *Inorg Chem*, 2007, **46**, 7163-7168.
14. S. V. Krivovichev, C. L. Cahill and P. C. Burns, *Inorg Chem*, 2003, **42**, 2459-2464.
15. G. Morrison, M. D. Smith and H.-C. zur Loye, *J Am Cheml Soc*, 2016, **138**, 7121-7129.
16. G. H. John, I. May, M. J. Sarsfield, H. M. Steele, D. Collison, M. Helliwell and J. D. McKinney, *Dalton Transac*, 2004, 734-740.
17. E. Strub, D. Groedler, D. Zaratti, C. R. C. Yong, L. Duennebier, S. Bazhenova, M. R. Jungfer, M. Breugst and M. Zegke, *Chem-Eur J*, 2024, e2024001.
18. a) B. P. Burton-Pye, I. Radivojevic, D. McGregor, I. M. Mbomekalle, W. W. Lukens, Jr. and L. C. Francesconi, *J Am Chem Soc*, 2011, **133**, 18802-18815; b) K. E. German, A. M. Fedoseev, M. S. Grigoriev, G. A. Kirakosyan, T. Dumas, C. Den Auwer, P. Moisy, K. V. Lawler, P. M. Forster and F. Poineau, *Chem-Eur J*, 2021, **27**, 13624-13631; cI. Denden, J. Roques, F. Poineau, P. L. Solari, M. L. Schlegel, G. Blain and M. Fattahi, *Radiochim Acta*, 2017, **105**, 135-140; dM. Zegke, D. Grödler, M. R. Jungfer, A. Haseloer, M. Kreuter, J. M. Neudörfl, T. Sittel, C. M. James, J. Rothe, M. Altmaier, A. Klein, M. Breugst, U. Abram, E. Strub and M. S. Wickleder, *Angew Chem Int Edit*, 2022, **61**.
19. P. Thuéry, *Inorgc Chem*, 2013, **52**, 435-447.
20. A. N. Alsobrook, B. G. Hauser, J. T. Hupp, E. V. Alekseev, W. Depmeier and T. E. Albrecht-Schmitt, *Chem Commun*, 2010, **46**, 9167-9169.
21. a) P. Thuéry, *EurJIC*, 2014, **2014**, 58-68; bG. Andreev, N. Budantseva, A. Levtsova, M. Sokolova and A. Fedoseev, *CrystEngComm*, 2020, **22**, 8394-8404; cP. Thuéry, *Crystal Growth & Design*, 2008, **8**, 4132-4143.
22. a) M. J. Abrams, S. K. Larsen and J. Zubieta, *Inorg Chem*, 1991, **30**, 2031-2035; bF. D. Rochon, R. Melanson and P.-C. Kong, *Acta Cryst C*, 1992, **48**, 785-788; cA. Davison, B. V. DePamphilis, A. G. Jones, K. J. Franklin and C. J. L. Lock, *Inorganica Chimica Acta*, 1987, **128**, 161-167.
23. a) D. McGregor, B. P. Burton-Pye, I. M. Mbomekalle, P. A. Aparicio, S. Romo, X. López, J. M. Poblet and L. C. Francesconi, *Inorg Chem*, 2012, **51**, 9017-9028; b) D. McGregor, B. P. Burton-Pye, R. C. Howell, I. M. Mbomekalle, W. W. Lukens, Jr., F. Bian, E. Mausolf, F. Poineau, K. R. Czerwinski and L. C. Francesconi, *Inorg Chem*, 2011, **50**, 1670-1681; c) A. Venturelli, M. J. Nilges, A. Smirnov, R. L. Belford and L. C. Francesconi, *J Chem Soc, Dalton Transactions*, 1999, 301-310.
24. J. De Yoreo, in *Crystallization via Nonclassical Pathways Volume 1: Nucleation, Assembly, Observation & Application*, American Chemical Society, 2020, vol. 1358, ch. 1, pp. 1-17.
25. W. Wang, L. B. Fullmer, N. A. G. Bandeira, S. Goberna-Ferrón, L. N. Zakharov, C. Bo, D. A. Keszler and M. Nyman, *Chem*, 2016, **1**, 887-901.